Ecology, 96(10), 2015, pp. 2590–2597

Reports

Animal movement constraints improve resource selection inference in the presence of telemetry error

Brian M. Brost,[1,5] Mevin B. Hooten,[2] Ephraim M. Hanks,[3] and Robert J. Small[4]

[1]*Department of Fish, Wildlife, and Conservation Biology, Colorado State University, Fort Collins, Colorado 80523 USA*
[2]*U.S. Geological Survey, Colorado Cooperative Fish and Wildlife Research Unit, Department of Fish, Wildlife, and Conservation Biology, Colorado State University, and Department of Statistics, Colorado State University, Fort Collins, Colorado 80523 USA*
[3]*Department of Statistics, Pennsylvania State University, University Park, Pennsylvania 16801 USA*
[4]*Division of Wildlife Conservation, Alaska Department of Fish and Game, Juneau, Alaska 99802 USA*

Abstract. Multiple factors complicate the analysis of animal telemetry location data. Recent advancements address issues such as temporal autocorrelation and telemetry measurement error, but additional challenges remain. Difficulties introduced by complicated error structures or barriers to animal movement can weaken inference. We propose an approach for obtaining resource selection inference from animal location data that accounts for complicated error structures, movement constraints, and temporally autocorrelated observations. We specify a model for telemetry data observed with error conditional on unobserved true locations that reflects prior knowledge about constraints in the animal movement process. The observed telemetry data are modeled using a flexible distribution that accommodates extreme errors and complicated error structures. Although constraints to movement are often viewed as a nuisance, we use constraints to simultaneously estimate and account for telemetry error. We apply the model to simulated data, showing that it outperforms common ad hoc approaches used when confronted with measurement error and movement constraints. We then apply our framework to an Argos satellite telemetry data set on harbor seals (*Phoca vitulina*) in the Gulf of Alaska, a species that is constrained to move within the marine environment and adjacent coastlines.

Key words: animal movement; Argos satellite; Bayesian hierarchical model; Gulf of Alaska; harbor seal; Phoca vitulina; *resource selection; spatial point process; telemetry error; temporal autocorrelation.*

Introduction

Conservation and management of animal populations requires knowledge of factors affecting their abundance and distribution. The locations of animals, coupled with information about associated environmental characteristics, can be used to quantify species–habitat relationships. This has stimulated the widespread use of telemetry devices to collect animal location data (hereafter telemetry data), which are often analyzed in a resource selection framework (Manly et al. 2002). The goal of such analyses is to quantify the probability of resource (or habitat) use conditional on resource availability (i.e., selection). Use that is disproportionate to availability is often equated with preference (Manly et al. 2002).

Multiple factors complicate the application of resource selection methodology. Modern satellite telemetry devices, for example, can collect multiple locations per day. Although such data increase the prospects for obtaining inference about animal behavior, they often violate the usual independence assumption of basic statistical analyses (Aarts et al. 2008, Fieberg et al. 2010). Telemetry measurement error poses another challenge. Measurement errors, or deviations between recorded telemetry locations and true animal locations, can interact with environmental heterogeneity to bias inferences on species–habitat relationships (Visscher 2006, Johnson and Gillingham 2008, Hefley et al. 2014).

Recent extensions to models for analyzing animal telemetry data address temporal autocorrelation and measurement error. Johnson et al. (2008*b*), for example, modeled temporally autocorrelated location data using a weighted distribution that combines a resource selection function with a movement model. Morales et al. (2004), Hooten et al. (2010), and Hanks et al. (2011) provide alternatives to the weighted distribution approach that also account for temporally dependent data. So-called "state-space" movement models further account for telemetry measurement error by coupling a statistical model for the telemetry observation process with a model that describes the true, but unobserved, movement process (Patterson et al. 2008). In principle, state-space movement models can be used to directly quantify species–habitat relationships (McClintock et al. 2012); however, they are typically used only to estimate true animal paths and infer behavioral states.

Manuscript received 14 March 2015; revised 22 May 2015; accepted 26 May 2015. Corresponding Editor: E. G. Cooch.
[5] E-mail: bmbrost@gmail.com

The contemporary methods highlighted here are important developments for the analysis of telemetry location data; however, additional challenges remain. For example, existing models assume elliptical (or circular) patterns of measurement error, even though some remote sensing devices impose more complicated error structures on the data. Constraints, or barriers, to animal movement present another complication. Constraints modify the spatial support of the animal movement process by limiting where an individual or species exists, and may interact with measurement error to yield telemetry locations that occur in areas not accessible by the telemetered individual (e.g., Fig. 1a). Although spatial constraints have been incorporated into animal movement models (e.g., Sumner et al. 2009, McClintock et al. 2012), they have not been used to quantify resource selection.

We propose an approach for obtaining inference concerning resource selection from animal location data that accounts for complicated error structures, constraints to animal movement, and temporally autocorrelated observations. To our knowledge, these objectives have not been addressed previously in a unified framework. We specify a model for observed telemetry data conditional on true, but unknown, locations that reflects prior knowledge about constraints on the animal movement process. Although constraints to animal movement are typically viewed as a nuisance, our approach uses constraints to simultaneously estimate and account for telemetry error. We first apply the model to a simulated data set and compare it to common ad hoc approaches used when confronted with constraints to animal movement. We also illustrate our framework by analyzing an Argos satellite telemetry data set on harbor seals (*Phoca vitulina*) in the Gulf of Alaska; this species is constrained to move within the marine environment and adjacent coastlines.

Telemetry Location Data

The model that we propose is general and can be applied to various combinations of telemetry data types (e.g., VHF, GPS, or geolocation telemetry); however, our focus here is on Argos telemetry data. Argos satellite telemetry is a popular platform for collecting animal location data because it is cost effective, and because all location estimates are conveniently delivered to the end user electronically, making tag recovery unnecessary. Argos satellite telemetry has also seen extensive use for more than two decades, resulting in massive historical data sets that are ripe for reanalysis using state-of-the-art methodology (Movebank.org currently contains >250 Argos telemetry data sets).

Our model application specifically focuses on telemetry locations like those in our harbor seal data set, which were calculated via the Argos least squares positioning algorithm (Service Argos 2015). These location data require special treatment because they exhibit an x-shaped error distribution that has greatest

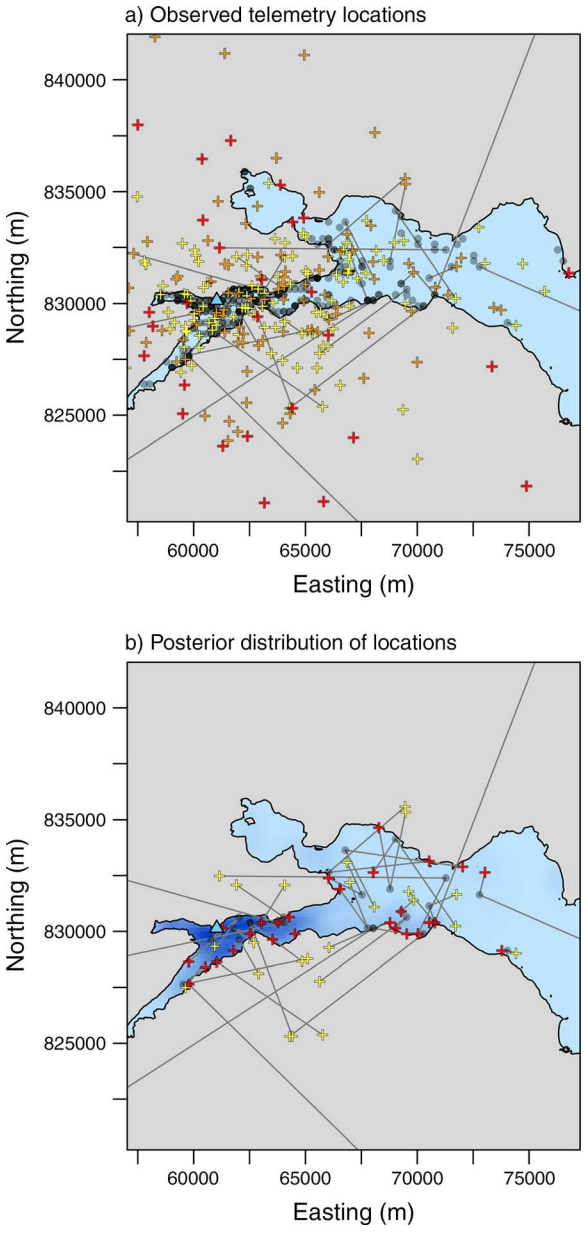

FIG. 1. Simulation of 300 true locations ($\boldsymbol{\mu}_t$, black circles) of harbor seals (*Phoca vitulina*) in the Gulf of Alaska, according to the process model (Eq. 3) using two resource selection covariates, namely distance to a point of attraction (e.g., a haul-out site; blue triangle) and bathymetry. The blue polygon represents S, the spatial support of the movement process within which all $\boldsymbol{\mu}_t$ occur. (a) Observed telemetry locations ($\mathbf{s}_t$; crosses) were simulated according to the observation model (Eq. 1) with three levels of telemetry measurement error corresponding to high- (yellow), medium- (orange), and low- (red) accuracy Argos locations (i.e., Argos location classes 3, 0, and B, respectively). The lines connect a subset of observed locations with their corresponding true location. (b) The posterior distribution of $\boldsymbol{\mu}_t$ (blue to purple color gradient in S; darker colors represent higher posterior probability). Lines connect a subset of true animal locations (black circles) with their corresponding observed locations (yellow crosses) and posterior modes (red crosses).

error variance along the NW–SE and NE–SW axes, a consequence of the polar orbiting Argos satellites and error that is largest in the direction perpendicular to the orbit (Costa et al. 2010, Douglas et al. 2012). Analysis of these data is further complicated by the fact that valid Argos telemetry locations are assigned one of six location classes, each exhibiting different error patterns and magnitudes. In order of decreasing accuracy, the location classes are 3, 2, 1, 0, A, and B.

Model Formulation

Suppose individuals in a population of animals are constrained to move within S, the spatial support of the movement process. Let $\mathbf{s}_t \equiv (s_{1,t}, s_{2,t})'$ be the pair of coordinates for an observed telemetry location on a single individual at time t, and $\boldsymbol{\mu}_t \equiv (\mu_{1,t}, \mu_{2,t})'$ be the pair of coordinates for the corresponding latent (i.e., unobserved) true location. Although $\boldsymbol{\mu}_t$ is restricted to be within S, this is not true for the observed telemetry location which can fall outside of S due to measurement error (Fig. 1a).

Observation model.—An appropriate observation model must describe how telemetry locations arise conditional on true locations. We allow for various telemetry error structures using

$$\mathbf{s}_t \sim \begin{cases} t_\nu(\boldsymbol{\mu}_t, \boldsymbol{\Sigma}), & \text{with probability } p_t \\ t_\nu(\boldsymbol{\mu}_t, \tilde{\boldsymbol{\Sigma}}), & \text{with probability } 1 - p_t \end{cases}. \quad (1)$$

In this expression, the observed telemetry locations $\mathbf{s}_t$ arise from a mixture of multivariate t distributions with mean $\boldsymbol{\mu}_t$ (the true location), scale matrices $\boldsymbol{\Sigma}$ and $\tilde{\boldsymbol{\Sigma}}$, and "degrees of freedom" ν. The parameters $\boldsymbol{\Sigma}$, $\tilde{\boldsymbol{\Sigma}}$, and ν describe error in the telemetry measurement process. The degrees of freedom parameter ν specifically adjusts the heaviness of the tails in the t distribution, thereby accommodating extreme errors commonly seen in telemetry data (Jonsen et al. 2005, Hoenner et al. 2012). Note that the t distribution approximates a Gaussian distribution for $\nu \geq 30$. The scale matrix $\boldsymbol{\Sigma}$ is parametrized in a flexible manner:

$$\boldsymbol{\Sigma} = \sigma^2 \begin{bmatrix} 1 & \rho\sqrt{a} \\ \rho\sqrt{a} & a \end{bmatrix} \quad (2)$$

where σ^2 quantifies scale in the longitude direction, a modifies σ^2 to describe scale in the latitude direction, and ρ describes the correlation between variation in the two directions. The scale matrix $\tilde{\boldsymbol{\Sigma}}$ is identical to $\boldsymbol{\Sigma}$ except for the off-diagonal elements which are multiplied by -1; thus, the off-diagonals of $\tilde{\boldsymbol{\Sigma}}$ are $-\rho\sqrt{a}$.

When $\rho = 0$, Eq. 1 collapses to a single multivariate t distribution that is appropriate for circular ($a = 1$) and elliptical error distributions ($a \neq 1$). Alternatively, $\rho \neq 0$ results in two distributions that are reflected across the vertical axis. Consequently, when $\rho \neq 0$, Eq. 1 specifies a mixture distribution that decomposes potentially complicated error structures like the x-shaped pattern evident in Argos telemetry data into two simpler forms, with one mixture component for errors along the NE–SW axis (described by $\boldsymbol{\Sigma}$) and another for errors along the SE–NW axis (described by $\tilde{\boldsymbol{\Sigma}}$). We define $p_t = 0.5$ because the orbital plane of Argos satellites changes continuously; therefore, observations are equally likely to come from either mixture component.

The parameters relating to measurement error (i.e., σ^2, ρ, a, and ν) can be estimated independently for different error classes (e.g., Argos location quality classes) or adapted to accommodate a continuous metric of location quality (e.g., GPS dilution of precision). Since 2011, Argos has also provided error ellipses associated with locations processed via a Kalman filtering algorithm. Error ellipses better characterize the magnitude and orientation of errors than location classes, and can be used to inform observation model parameters (e.g., McClintock et al. 2014).

Process model.—Animal locations are naturally viewed as a realization of a point process that has a spatially heterogeneous intensity function (Aarts et al. 2012, Johnson et al. 2013). The intensity function summarizes the ecological processes that give rise to animal locations, and thus provides inference for species–habitat relationships. A weighted distribution is often used to model this intensity function (Lele and Keim 2006, Aarts et al. 2012), which is the approach we adopt as a model for the true locations:

$$\boldsymbol{\mu}_t \sim \frac{\exp\{\mathbf{x}'(\boldsymbol{\mu}_t)\boldsymbol{\beta} - \eta(\boldsymbol{\mu}_t, \boldsymbol{\mu}_{t-\Delta_t})\}}{\int_S \exp\{\mathbf{x}'(\boldsymbol{\mu})\boldsymbol{\beta} - \eta(\boldsymbol{\mu}, \boldsymbol{\mu}_{t-\Delta_t})\} d\boldsymbol{\mu}}. \quad (3)$$

In Eq. 3, $\mathbf{x}(\boldsymbol{\mu}_t)$ is a vector of spatially referenced resource or habitat covariates at location $\boldsymbol{\mu}_t$, $\boldsymbol{\beta}$ is a vector of resource selection coefficients, and $\eta(\boldsymbol{\mu}_t, \boldsymbol{\mu}_{t-\Delta_t})$ is a spatially explicit movement kernel centered at $\boldsymbol{\mu}_{t-\Delta_t}$, the previous true location (Δ_t denotes the time elapsed between $\boldsymbol{\mu}_t$ and the previous true location). We approximate the integral in the denominator of Eq. 3 by numerical quadrature (Dorazio 2012). The kernel $\eta(\boldsymbol{\mu}_t, \boldsymbol{\mu}_{t-\Delta_t})$ governs the distribution of available habitat and accounts for temporal autocorrelation among locations. The movement kernel is modeled as

$$\eta(\boldsymbol{\mu}_t, \boldsymbol{\mu}_{t-\Delta_t}) = \frac{d(\boldsymbol{\mu}_t, \boldsymbol{\mu}_{t-\Delta_t})}{\Delta_t \phi} \quad (4)$$

where $d(\boldsymbol{\mu}_t, \boldsymbol{\mu}_{t-\Delta_t})$ is the distance between $\boldsymbol{\mu}_t$ and $\boldsymbol{\mu}_{t-\Delta_t}$, and ϕ is a scaling parameter. Importantly, $d(\cdot, \cdot)$ must adhere to animal movement constraints and is thus measured exclusively through the domain defined by S. In the case of marine mammals like harbor seals, $d(\cdot, \cdot)$ represents the distance through water (i.e., the swim distance). In practice, we calculate $d(\cdot, \cdot)$ using least-cost distance (Dijkstra 1959). Given that Eq. 4 takes the form of an exponential kernel, the range of correlation between consecutive locations can be inferred by noting that $\eta(\boldsymbol{\mu}_t, \boldsymbol{\mu}_{t-\Delta_t}) \approx 0$ when $d(\boldsymbol{\mu}_t, \boldsymbol{\mu}_{t-\Delta_t})/\Delta_t > 3\phi$.

TABLE 1. Performance of five methods for estimating $\boldsymbol{\mu}_t$ (true locations) based on 250 simulations of 1000 telemetry locations each.

	All locations		High-accuracy locations		Medium-accuracy locations		Low-accuracy locations	
Estimation method	$E(n)$	$E(d)$ (m)	$E(n)$	$E(d)$ (m)	$E(n)$	$E(d)$ (m)	$E(n)$	$E(d)$ (m)
Mixture t model	1000	2178	333	1811	334	2208	333	2513
Snap $\mathbf{s}_t$ to S	1000	10890	333	3173	334	6108	333	23393
Exclude $\mathbf{s}_t \notin S$	326	9867	160	2715	125	4416	40	22472
Speed filter	211	4971	117	2460	83	3116	11	9357
Normal model	1000	2615	333	2162	334	2778	333	2905

Notes: The notation $E(\cdot)$ denotes the expectation, or mean value over the simulations. Specifically, $E(n)$ is the expected sample size and $E(d)$ represents $E[d(\hat{\boldsymbol{\mu}}_t, \boldsymbol{\mu}_t)]$, the expected distance in meters between $\hat{\boldsymbol{\mu}}_t$ (the estimated true location) and $\boldsymbol{\mu}_t$ as measured through the domain defined by S. For the mixture t and normal models, $\hat{\boldsymbol{\mu}}_t$ was calculated as Mode($\boldsymbol{\mu} \mid \mathbf{s}$). The expected distance $E[d(\hat{\boldsymbol{\mu}}_t, \boldsymbol{\mu}_t)]$ for all locations combined was weighted to account for varying sample sizes in the exclude $\mathbf{s}_t \notin S$ and speed filter methods. High-, medium-, and low-accuracy observed locations were simulated to be consistent with Argos location classes 3, 0, and B, respectively.

Prior distributions.—To complete the Bayesian formulation of this model, we specify prior distributions for the unknown parameters. We assume $\sigma \sim \text{Uniform}(0, u)$ with similar uniform priors for ρ, a, ν, and ϕ, and $\boldsymbol{\beta} \sim \text{N}(\mathbf{0}, \tau^2\mathbf{I})$, where τ^2 is the variance and $\mathbf{I}$ represents the identity matrix. See Appendix A for the full model specification and Appendix B for details regarding model implementation.

Model Application

Model evaluation using simulated data

An example realization from the model described above is shown in Fig. 1a. All parameters in the simulation were chosen to be similar to those estimated in an analysis of harbor seal telemetry data (see *Case study*). To simplify presentation of results, telemetry measurement error corresponded to high-, medium-, and low-accuracy Argos locations (i.e., location classes 3, 0, and B, respectively).

We fit the model using a Markov chain Monte Carlo (MCMC) algorithm written in R (provided in the Supplement; R Development Core Team 2013) to 250 data sets simulated using the process previously described, each containing 1000 locations randomly allocated to the three error classes. Inference was based on 2000 MCMC samples after convergence. An example of posterior inference for the true locations $\boldsymbol{\mu}_t$ is shown in Fig. 1b.

We compare inference for $\boldsymbol{\mu}_t$ and $\boldsymbol{\beta}$ from our model to three ad hoc alternatives commonly used when confronted with telemetry measurement error and constraints to animal movement. These alternative approaches approximate $\boldsymbol{\mu}_t$ by (1) "snapping" observed telemetry locations to the nearest location in S; (2) excluding from analysis all observed locations not in S; or (3) using a speed filter (Freitas et al. 2008) to first remove particularly aberrant observations, then eliminating remaining observations that are not in S. A spatial point process model is then used for resource selection inference (Aarts et al. 2012). Specifically, we modeled the counts of $\boldsymbol{\mu}_t$ per spatial unit (e.g., raster grid cell) using a Poisson generalized linear model. We make one additional comparison with a model wherein Eq. 1 is updated to be a normal distribution with $\rho = 0$. This modification mimics the simpler observation models commonly used in other approaches (e.g., Jonsen et al. 2003, Johnson et al. 2008*a*, Sumner et al. 2009) and provides a benchmark for assessing the performance of a mixture model that accommodates complicated error distributions.

Inference pertaining to the latent state variable $\boldsymbol{\mu}_t$ and resource selection coefficients $\boldsymbol{\beta}$ from the approaches just described are summarized in Tables 1 and 2. Our model retains all telemetry locations to estimate $\boldsymbol{\mu}_t$ with greater accuracy than the alternative approaches, and particularly excels for the lower quality error classes that often dominate animal telemetry data sets (Douglas et al. 2012). Censoring observations (ad hoc alternatives 2 and 3) eliminated >66% of the observed locations; data loss was particularly severe for the lower quality error classes. Estimates of $\boldsymbol{\beta}$ were overly confident when $\boldsymbol{\mu}_t$ was approximated by filtering, snapping telemetry locations to S, or excluding observations not in S (Table 2). For example, interval coverage for one of the resource selection coefficients was 0% for all of these approaches. Coverage of intervals for the mixture t model was comparable to coverage attained when Eq. 1 was updated to a bivariate normal observation model. Both provided nominal coverage for $\boldsymbol{\beta}$, as well as estimates of $\boldsymbol{\beta}$ that were the least biased among all approaches (Table 2). Estimates of other parameters in our model were satisfactory and are described in detail in Appendix C.

Case study: Harbor seals

To demonstrate our approach with real data, we applied our model to telemetry locations of an adult female harbor seal monitored near Kodiak Island, Alaska during 1995 and 1996 (Fig. 2). Telemetry locations were collected on average every 4.3 h (range 0.02–131.9 h) using an Argos satellite telemetry device. The animal's position was measured on 1457 occasions, with ~80% of locations coming from the three least accurate Argos location classes (i.e., large measurement error). We used a 250-m resolution raster of the marine environment to define S, the extent of which was limited to 60 km (measured through the water) from the haul-

TABLE 2. Performance of five methods for estimating $\boldsymbol{\beta}$ (resource selection coefficients) based on 250 simulations of 1000 telemetry locations each.

	Distance to haul-out, β_1		Bathymetry, β_2	
Estimation method	Relative bias	Coverage	Relative bias	Coverage
Mixture t model	0.01	0.96	0.01	0.90
Snap $\mathbf{s}_t$ to S	−0.33	0.00	0.02	0.83
Exclude $\mathbf{s}_t \notin S$	−0.05	0.63	−0.94	0.00
Speed filter	0.28	0.10	−0.92	0.00
Normal model	0.02	0.92	0.02	0.85

Notes: Relative bias in estimating $\boldsymbol{\beta}$ was calculated as $(E(\boldsymbol{\beta}) - \boldsymbol{\beta})/\boldsymbol{\beta}$ and "Coverage" is the percentage of 95% intervals that contained the true $\boldsymbol{\beta}$.

out location. Defining S in this way should capture all potential $\boldsymbol{\mu}_t$ because harbor seals typically stay within 30 km of their haul-outs (Lowry et al. 2001, Small et al. 2005), and nothing suggests that this individual exhibited longer distance movements. For illustration purposes, we focused on selection inference pertaining to distance to haul-out site and bathymetry. Both covariates were represented as 250-m resolution rasters and were only marginally correlated ($r = 0.14$).

Point estimates for $\boldsymbol{\mu}_t$ (posterior mode) were 4.2 km from the haul-out site, on average, and 95% of the posterior probability for $\boldsymbol{\mu}_t$ was within 13.0 km of the haul-out site in water 55 m deep or less (Fig. 2). Resource selection coefficients for distance to haul-out and bathymetry were estimated as $\beta_1 = -2.03$ (95% CI: −2.45, −1.62) and $\beta_2 = -0.82$ (95% CI: −1.12, −0.53), respectively, indicating that areas far from the haul-out site and deeper water were selected against. These results are consistent with other findings that harbor seals generally use shallower water near their haul-out sites (Lowry et al. 2001, Small et al. 2005). Estimates for ν were less than 30 for all Argos error classes, supporting our use of the t distribution to ensure that extreme observations do not exert undue influence on inferences. Estimates for all parameters are provided in Appendix D and we illustrate the flexibility of our observation

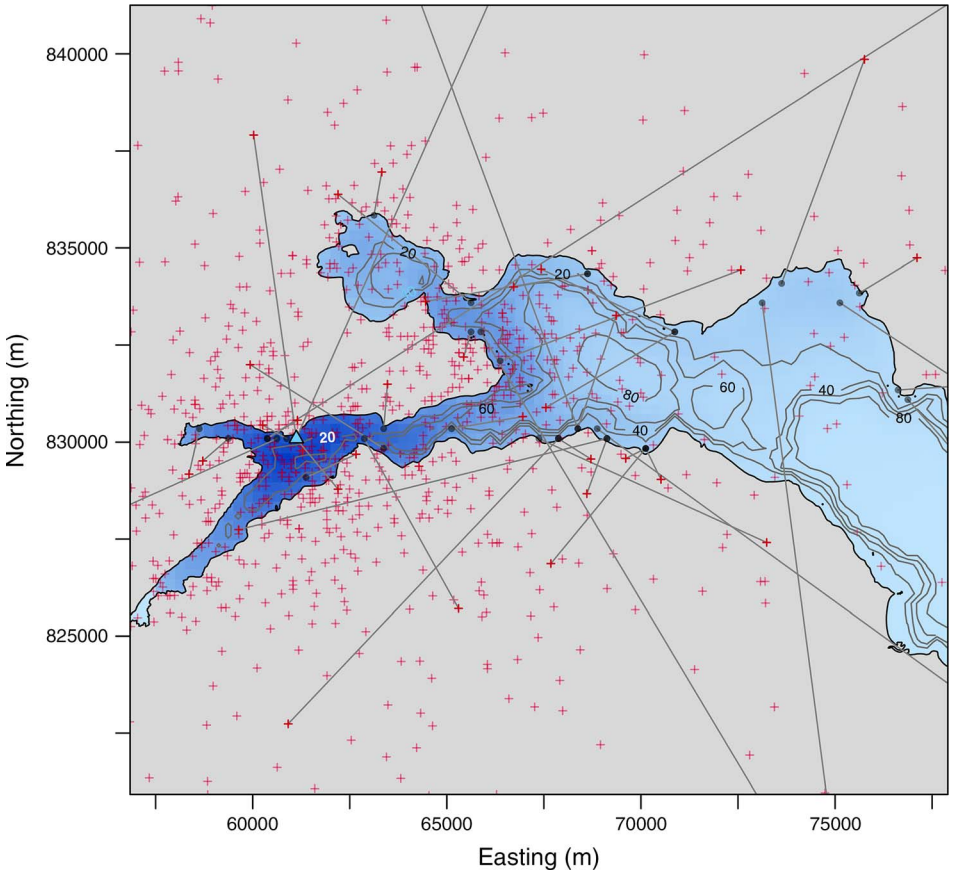

FIG. 2. Argos satellite telemetry locations (red crosses) of an adult female harbor seal monitored from 9 October 1995 to 4 June 1996 along the southern coast of Kodiak Island, Alaska, USA. The blue polygon represents S, the spatial support of the movement process; for seals, this is the marine environment and adjacent coastlines. Our analysis focused on resource selection inference pertaining to distance to haul-out site (blue triangle) and bathymetry (gray contour lines). The posterior distribution of $\boldsymbol{\mu}_t$ is represented by the blue to purple color gradient in S; darker colors indicate higher posterior probability. Lines connect a subset of observed locations with their corresponding posterior modes (black circles). Water depth contours are labeled in meters.

model in Appendix E. All inference was based on 100 000 MCMC samples, which required 55 hours of processing time on a computer equipped with a 3.0 GHz Intel Xeon processor.

Discussion

Our model for resource selection inference addresses several complicating factors in the analysis of animal telemetry data. Our model accounts for telemetry measurement error and temporally autocorrelated observations, and, unlike other approaches, also accommodates complicated error structures and constraints to animal movement. In fact, we show that constraints to movement are helpful in estimating and accounting for measurement error.

Our model consists of two general components, one "process" model for the true animal locations and another for the observed telemetry locations that is conditional on the true locations (the "observation" model). These components are implemented in a unified framework such that uncertainty naturally propagates through the model, thereby properly accounting for uncertainty in parameter estimates. This unification further allows resource or habitat covariates to improve estimation of $\boldsymbol{\mu}_t$. Methods that are implemented in two stages, where the true locations are first estimated and then used in a secondary analysis to quantify resource selection, do not allow uncertainty in the first stage to propagate through the second stage unless a bootstrapping or multiple imputation procedure is used (e.g., Hanks et al. 2011). The ad hoc alternatives presented in our simulation study bear this shortcoming, as do state-space movement models, which are often applied in a two-step fashion. Our framework also allows for generalizations such as the joint analysis of multiple individuals using random effects for $\boldsymbol{\beta}$ and ϕ, which could themselves be functions of auxiliary demographic information such as gender or age.

Methods that account for sampling artifacts improve ecological inference. Ignoring telemetry measurement errors, or hiding them in a pre-processing stage, yields inaccurate estimates of true animal locations and inference for resource selection coefficients that is biased and overly confident (Tables 1 and 2). Censoring poor-quality locations leads to substantial data loss, particularly when dealing with wildlife data sets that often largely consist of low-quality observations (Douglas et al. 2012). Given the x-shaped error pattern in Argos telemetry data, true animal locations are more likely to occur on a diagonal from the observed location, rather than, for example, due north of the observed location. Our observation model incorporates this nuance and estimates $\boldsymbol{\mu}_t$ with greater accuracy than one that assumes simpler, elliptical error structures (Table 1). However, both approaches account for uncertainty in $\boldsymbol{\mu}_t$ and thus provided comparable inference for $\boldsymbol{\beta}$.

Animal behavior, such as increased milling by harbor seals near haul-out sites, can bias times at which satellite telemetry locations are acquired and may therefore affect resource selection inference (Frair et al. 2010). The telemetry device used in our case study was programmed to suspend transmissions after 6 h during haul-out bouts, mitigating this concern. Alternatively, predicting $\boldsymbol{\mu}_t$ at a fixed time interval may account for bias (e.g., McClintock et al. 2012, 2013), although this general technique appears to be untested. Nonetheless, augmenting our model to obtain predictions for unobserved $\boldsymbol{\mu}_t$ at any time or sequence of times is straightforward. However, methods that are conceptually based on locations collected at regular time intervals may not be applicable when data are as intermittent as those in our harbor seal data set (Breed et al. 2011, Silva et al. 2014). Methods for point process data collected under preferential sampling present another promising option for modeling temporally biased telemetry locations (Diggle et al. 2010).

Constraints in space and time

Many animals such as African elephants, European bison, Asiatic wild asses, and Mongolian gazelles encounter fences, railroads, roads, and other barriers that prevent free-ranging movements (Loarie et al. 2009, Kowalczyk et al. 2012, Ito et al. 2013). Our model could easily be extended to accurately estimate the locations of these species in their spatially constrained environments. Features that restrict but do not preclude movement, such as proximity to water, a nest site, or escape terrain, also represent constraints. These "soft" constraints can be modeled in much the same way as we modeled attraction to a haul-out site for harbor seals (i.e., as a component of the resource selection function).

Methods that account for measurement error, such as state-space movement models, often require an a priori understanding of error patterns, usually obtained from published studies (Jonsen et al. 2003, Jonsen et al. 2005, Johnson et al. 2008*a*). Unfortunately, observed error patterns can differ in unpredictable ways due to differences in animal behavior, habitat obstructions, environmental conditions, and geographic locations (Cargnelutti et al. 2007, Lewis et al. 2007, Douglas et al. 2012). Consequently, no single description of measurement error may be universally applicable to a tracking technology. Constraints to movement, and the subsequent discrepancy between the spatial support of $\boldsymbol{\mu}_t$ and $\mathbf{s}_t$, allow our model to estimate species- and system-specific telemetry measurement error without the expense of collecting additional data (e.g., Costa et al. 2010 and Douglas et al. 2012, who used two telemetry technologies to simultaneously collect locations on free-ranging animals). As such, we view constraints as an aid in the modeling and estimation process.

A second constraint, namely a mechanistic temporal movement constraint (Eq. 4), also operates in our model. This movement kernel expands and contracts inversely with Δ_t, thereby accounting for temporal autocorrelation between consecutive locations (Aarts et al. 2008, Johnson et al. 2008*b*, Forester et al. 2009,

Hooten et al. 2014). The kernel also defines the distribution of resources available to the individual, which is data-driven as it is governed by the estimated scale parameter ϕ and the previous location $\boldsymbol{\mu}_{t-\Delta t}$. The process model (Eq. 3) balances the effect of $\eta(\boldsymbol{\mu}_t, \boldsymbol{\mu}_{t-\Delta_t})$ with that of the resource selection function; both are modified by the spatial constraint when $\boldsymbol{\mu}_{t-\Delta_t}$ is near the boundary of S.

Guidance

Methods that accommodate barriers to movement are important for obtaining reliable inference on animals living in highly constrained environments; however, such methods are computationally expensive compared to alternatives that do not incorporate movement constraints (e.g., Johnson et al. 2008*a*). Future work comparing approaches, as well as varying degrees of constrained movements, will help to provide additional guidance. We encourage researchers to model the mechanisms affecting their measurements. Other ecological models have emphasized the observation process with much success (e.g., models for occupancy and capture–recapture abundance estimation). Analyses of telemetry data merit the same attention.

Acknowledgments

We thank two anonymous referees for helpful reviews of the manuscript. Our research was funded by the Alaska Department of Fish and Game (ADF&G), through award NA11NMF4390200 from the U.S. National Oceanic and Atmospheric Administration Fisheries, Alaska Region to the ADF&G. Any use of trade, firm, or product names is for descriptive purposes only and does not imply endorsement by the U.S. Government.

Literature Cited

Aarts, G., J. Fieberg, and J. Matthiopoulos. 2012. Comparative interpretation of count, presence–absence and point methods for species distribution models. Methods in Ecology and Evolution 3:177–187.

Aarts, G., M. MacKenzie, B. McConnell, M. Fedak, and J. Matthiopoulos. 2008. Estimating space-use and habitat preference from wildlife telemetry data. Ecography 31:140–160.

Breed, G. A., D. P. Costa, M. E. Goebel, and P. W. Robinson. 2011. Electronic tracking tag programming is critical to data collection for behavioral time-series analysis. Ecosphere 2: art10.

Cargnelutti, B., A. Coulon, A. J. M. Hewison, M. Goulard, J. Angibault, and N. Morellet. 2007. Testing global positioning system performance for wildlife monitoring using mobile collars and known reference points. Journal of Wildlife Management 71:1380–1387.

Costa, D. P., et al. 2010. Accuracy of Argos locations of pinnipeds at-sea estimated using Fastloc GPS. PLoS ONE 5: e8677.

Diggle, P. J., R. Menezes, and T. Su. 2010. Geostatistical inference under preferential sampling. Journal of the Royal Statistical Society C (Applied Statistics) 59:191–232.

Dijkstra, E. 1959. A note on two problems in connection with graphs. Numerische Mathematik 1:269–271.

Dorazio, R. M. 2012. Predicting the geographic distribution of a species from presence-only data subject to detection errors. Biometrics 68:1303–1312.

Douglas, D. C., R. Weinzierl, S. C. Davidson, R. Kays, M. Wikelski, and G. Bohrer. 2012. Moderating Argos location errors in animal tracking data. Methods in Ecology and Evolution 3:999–1007.

Fieberg, J., J. Matthiopoulos, M. Hebblewhite, M. S. Boyce, and J. L. Frair. 2010. Correlation and studies of habitat selection: problem, red herring or opportunity? Philosophical Transactions of the Royal Society B 365:2233–2244.

Forester, J. D., H. K. Im, and P. J. Rathouz. 2009. Accounting for animal movement in estimation of resource selection functions: sampling and data analysis. Ecology 90:3554–3565.

Frair, J. L., J. Fieberg, M. Hebblewhite, F. Cagnacci, N. J. DeCesare, and L. Pedrotti. 2010. Resolving issues of imprecise and habitat-biased locations in ecological analyses using GPS telemetry data. Philosophical Transactions of the Royal Society B 365:2187–2200.

Freitas, C., C. Lydersen, M. A. Fedak, and K. M. Kovacs. 2008. A simple new algorithm to filter marine mammal Argos locations. Marine Mammal Science 24:315–325.

Hanks, E. M., M. B. Hooten, D. S. Johnson, and J. T. Sterling. 2011. Velocity-based movement modeling for individual and population level inference. PLoS ONE 6:e22795.

Hefley, T. J., D. M. Baasch, A. J. Tyre, and E. E. Blankenship. 2014. Correction of location errors for presence-only species distribution models. Methods in Ecology and Evolution 5: 207–214.

Hoenner, X., S. D. Whiting, M. A. Hindell, and C. R. McMahon. 2012. Enhancing the use of Argos satellite data for home range and long distance migration studies of marine animals. PLoS ONE 7:e40713.

Hooten, M. B., E. M. Hanks, D. S. Johnson, and M. W. Alldredge. 2014. Temporal variation and scale in movement-based resource selection functions. Statistical Methodology 17:82–98.

Hooten, M. B., D. S. Johnson, E. M. Hanks, and J. H. Lowry. 2010. Agent-based inference for animal movement and selection. Journal of Agricultural, Biological, and Environmental Statistics 15:523–538.

Ito, T. Y., B. Lhagvasuren, A. Tsunekawa, M. Shinoda, S. Takatsuki, B. Buuveibaatar, and B. Chimeddorj. 2013. Fragmentation of the habitat of wild ungulates by anthropogenic barriers in Mongolia. PLoS ONE 8:e56995.

Johnson, C. J., and M. P. Gillingham. 2008. Sensitivity of species-distribution models to error, bias, and model design: an application to resource selection functions for woodland caribou. Ecological Modelling 213:143–155.

Johnson, D. S., M. B. Hooten, and C. E. Kuhn. 2013. Estimating animal resource selection from telemetry data using point process models. Journal of Animal Ecology 82: 1155–1164.

Johnson, D. S., J. M. London, M.-A. Lea, and J. W. Durban. 2008*a*. Continuous-time correlated random walk model for animal telemetry data. Ecology 89:1208–1215.

Johnson, D. S., D. L. Thomas, J. M. Ver Hoef, and A. Christ. 2008*b*. A general framework for the analysis of animal resource selection from telemetry data. Biometrics 64:968–976.

Jonsen, I. D., J. M. Flemming, and R. A. Myers. 2005. Robust state-space modeling on animal movement data. Ecology 86: 2874–2880.

Jonsen, I. D., R. A. Myers, and J. M. Flemming. 2003. Meta-analysis of animal movement using state-space models. Ecology 84:3055–3063.

Kowalczyk, R., K. Schmidt, and W. Jedrzejewski. 2012. Do fences or humans inhibit the movements of large mammals in Bialowieza Primeval Forest. Pages 235–244 *in* M. J. Somers and M. W. Hayward, editors. Fencing for conservation? Springer, New York, New York, USA.

Lele, S. R., and J. L. Keim. 2006. Weighted distributions and estimation of resource selection probability functions. Ecology 87:3021–3028.

Lewis, J. S., J. L. Rachlow, E. O. Garton, and L. A. Vierling. 2007. Effects of habitat on GPS collar performance: using data screening to reduce location error. Journal of Applied Ecology 44:663–671.

Loarie, S. R., R. J. V. Aarde, and S. L. Pimm. 2009. Fences and artificial water affect African savannah elephant movement patterns. Biological Conservation 142:3086–3098.

Lowry, L. F., K. J. Frost, J. M. Ver Hoef, and R. A. Delong. 2001. Movements of satellite-tagged subadult and adult harbor seals in Prince William Sound, Alaska. Marine Mammal Science 17:835–861.

Manly, B., L. McDonald, D. Thomas, T. L. McDonald, and W. P. Erickson. 2002. Resource selection by animals: statistical design and analysis for field studies. Kluwer, Dordrecht, The Netherlands.

McClintock, B. T., R. King, L. Thomas, J. Matthiopoulos, B. J. McConnell, and J. M. Morales. 2012. A general discrete-time modeling framework for animal movement using multistate random walks. Ecological Monographs 82:335–349.

McClintock, B. T., J. M. London, M. F. Cameron, and P. L. Boveng. 2014. Modelling animal movement using the Argos satellite telemetry location error ellipse. Methods in Ecology and Evolution 6:266–277.

McClintock, B. T., D. J. F. Russell, J. Matthiopoulos, and R. King. 2013. Combining individual animal movement and ancillary biotelemetry data to investigate population-level activity budgets. Ecology 94:838–849.

Morales, J. M., D. T. Haydon, J. Frair, K. E. Holsiner, and J. M. Fryxell. 2004. Extracting more out of relocation data: building movement models as mixtures of random walks. Ecology 85:2436–2445.

Patterson, T., L. Thomas, C. Wilcox, O. Ovaskainen, and J. Matthiopoulos. 2008. State-space models of individual animal movement. Trends in Ecology and Evolution 23:87–94.

R Development Core Team. 2013. R: a language and environment for statistical computing. R Foundation for Statistical Computing, Vienna, Austria. http://www.r-project.org/

Service Argos. 2015. Argos user's manual. CLS (Collecte Localization Satelites), Ramonville Saint-Agne, France. http://www.argos-system.org

Silva, M. A., I. Jonsen, D. J. F. Russell, R. Prieto, D. Thompson, and M. F. Baumgartner. 2014. Assessing performance of Bayesian state-space models fit to Argos satellite telemetry locations processed with Kalman filtering. PLoS ONE 9:e92277.

Small, R. J., L. F. Lowry, J. M. Ver Hoef, K. J. Frost, R. A. Delong, and M. J. Rehberg. 2005. Differential movements by harbor seal pups in contrasting Alaska environments. Marine Mammal Science 21:671–694.

Sumner, M. D., S. J. Wotherspoon, and M. A. Hindell. 2009. Bayesian estimation of animal movement from archival and satellite tags. PLoS ONE 4:e7324.

Visscher, D. 2006. GPS measurement error and resource selection functions in a fragmented landscape. Ecography 29:458–464.

Supplemental Material

Ecological Archives

Appendices A–E and the Supplement are available online: http://dx.doi.org/10.1890/15-0472.1.sm